Ferroelectrically tunable magnetism in BiFeO3/BaTiO3 heterostructure revealed by the first-principles calculations

Wenxuan Wang

Wei Sun

Guangbiao Zhang

Fengzhu Ren

Yuanxu Wang

See next page for additional authors

Recommended Citation

Ferroelectrically tunable magnetism in BiFeO3/BaTiO3 heterostructure revealed by the first-principles calculations

Abstract

© 2020 The perovskite oxide interface has attracted extensive attention as a platform for achieving strong coupling between ferroelectricity and magnetism. In this work, robust control of magnetoelectric (ME) coupling in the BiFeO3/BaTiO3 (BFO/BTO) heterostructure (HS) was revealed by using the first-principles calculation. Switching of the ferroelectric polarization of BTO induce large ME effect with significant changes on the magnetic ordering and easy magnetization axis, making up for the weak ME coupling effect of single-phase multiferroic BFO. In addition, the Dzyaloshinskii-Moriya interaction (DMI) and the exchange coupling constants J for the BFO part of the HSs are simultaneously manipulated by the ferroelectric polarization, especially the DMI at the interface is significantly enhanced, which is three or four times larger than that of the individual BFO bulk. This work paves the way for designing new nanomagnetic devices based on the substantial interfacial ME effect.

Keywords

Disciplines

Engineering | Physical Sciences and Mathematics

Publication Details

Authors

Wenxuan Wang, Wei Sun, Guangbiao Zhang, Fengzhu Ren, Yuanxu Wang, Caiyin You, and Zhenxiang Cheng

Ferroelectrically tunable magnetism in BiFeO$_3$/BaTiO$_3$ heterostructure revealed by the first-principles calculations

Wenxuan Wang [a], Wei Sun [a], Guangbiao Zhang [a], Fengzhu Ren [a], Yuanxu Wang [a,b], Caiyin You [c], Zhenxiang Cheng [a,d],[*]

[a] Institute for Computational Materials Science, School of Physics and Electronics, Henan University, Kaifeng 475004, People's Republic of China
[b] National Demonstration Center for Experimental Physics and Electronics Education, School of Physics, Henan University, Kaifeng 475004, People's Republic of China
[c] School of Materials Science & Engineering, Xi'an University of Technology, Xi'an 710048, People's Republic of China
[d] Institute for Superconducting & Electronic Materials, Australian Institute of Innovative Materials, University of Wollongong, Innovation Campus, Squires Way, North Wollongong, NSW 2500, Australia

GRAPHICAL ABSTRACT
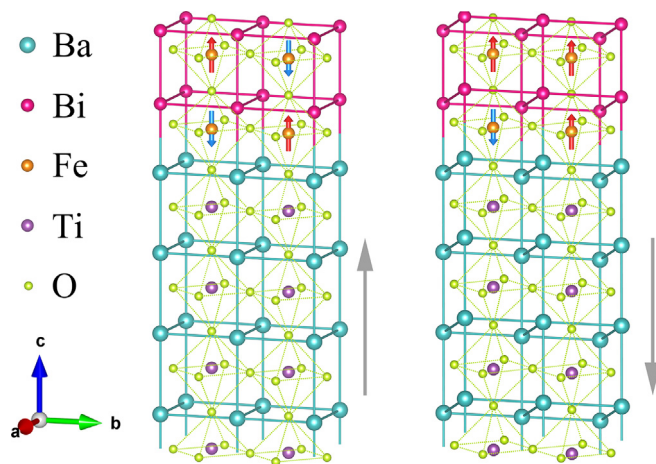
ARTICLE INFO

ABSTRACT

The perovskite oxide interface has attracted extensive attention as a platform for achieving strong coupling between ferroelectricity and magnetism. In this work, robust control of magnetoelectric (ME) coupling in the BiFeO$_3$/BaTiO$_3$ (BFO/BTO) heterostructure (HS) was revealed by using the first-principles calculation. Switching of the ferroelectric polarization of BTO induce large ME effect with significant changes on the magnetic ordering and easy magnetization axis, making up for the weak ME coupling effect of single-phase multiferroic BFO. In addition, the Dzyaloshinskii-Moriya interaction (DMI) and the exchange coupling constants *J* for the BFO part of the HSs are simultaneously manipulated by the ferroelectric polarization, especially the DMI at the interface is significantly enhanced, which is

Ferroelectric polarization
Magnetism

three or four times larger than that of the individual BFO bulk. This work paves the way for designing new nanomagnetic devices based on the substantial interfacial ME effect.

Introduction

Multiferroics, with simultaneous ferroelectric (FE) and ferromagnetic (FM) or ferroelastic properties, serves as the attractive candidate for realization of coupling among electrical, magnetic, and structural order parameters [1–5]. These compounds have potential applications such as nonvolatile memories, spintronic devices and sensors [6,7]. One of the technological attractions of the multiferroics lies in the ability to control magnetism by using electric field [6,8,9]. Of particular importance for such control is to be realized at room temperature for practical application. Among all single phase multiferroic materials, $BiFeO_3$ (BFO) take the great advantage with clear magnetoelectric (ME) coupling effect at room temperature [10,11]. This widely studied Type-I multiferroics [1] has large FE polarization, and weak magnetic moment due to spin spiral cycloid structure, magnetic and ferroelectric ordering temperatures much higher than room temperature, T_N = 643 k and T_C = 1103 k, respectively [12–15]. However, there is a relatively weak coupling between the magnetic and ferroelectric orders in the BFO due to the different ions origin for FM and FE, and to maintain its advantages but enhance its ME coupling would be a fundamental challenge. Intriguingly, the epitaxial oxide heterostructure (HSs) provides a fertile playground to enhance the ME effect and manipulate the corresponding electronic and magnetic properties of the structure [16–18].

The magnetic and ferroelectric orders coupling of BFO is partially connected by Dzyaloshinskii-Moriya interaction (DMI). The DMI is a chiral energy term derived from both spin–orbit coupling and inversion symmetry breaking, which is a relativistic correction of superexchange interactions [19–23]. DMI can cause attractive magnetic phenomena, examples including Skyrmions [24,25], domain wall dynamics [26,27], and spiral spin texture [28,29]. Recently, increasing reports have been focused on the relevant explanations and discussions of DMI, including methods to change the DMI sign and magnitude or the ways to enhance the DMI [30–33], as well as the potential applications driven by DMI effects [34,35]. For example, DMI can be enhanced by the increased magnetization in high strained BFO films through the reinforced electrical stimulation [36]. In addition, the enhanced Ferromagnetism (FM) and ferroelectricity (FE) of epitaxial BFO films on the $SrTiO_3$ substrates experimentally prepared by laser pulse deposition (PLD) are attributed to the DMI [37]. Of particular interest is that magnetic skyrmion have been observed in various epitaxial oxide HSs driven by DMI [38–40], e.g. the recently reported of $BaTiO_3$ (BTO)/$SrRuO_3$ HSs. Successful manipulation of skyrmion with the contribution of the DMI in such HS has enabled novel applications both for small size and electrically controllable spintronic device [41]. The investigation of these epitaxial systems suggest greater flexibility and possibility of coupling between ferroelectricity and magnetism via DMI effect in artificially designed HSs interfaces.

Although many theoretical and experimental investigations have been carried out on the BFO/BTO superlattice structure, especially the exploration and research on its ME coupling coefficient [42–47], ferroelectric properties [48,49] and the photovoltaic characteristics [50,51], the related theoretical researches about ferroelectrically tunable magnetic properties are still lacking in its HSs system. In addition, HSs generally have better growth stability than superlattice, and the former can easily achieve switchability and controllability of ferroelectric polarization by applying an external

electric field on the substrate, thus achieving effective control of the magnetic properties, including the DMI. Here, we designed a BTO/BFO HSs using first-principles calculations to explore ME coupling effect by the tunable ferroelectric polarization of BTO. Such HSs demonstrate ferroelectrically controllable magnetism, i.e. the tuning of antiferromagnetism (AFM) to FM, as well as the switching of easy magnetization between the in-plane and out-of-plane axis. In addition, the interfacial DMI magnitude of the HSs is three or four times larger than that of the BFO bulk with the presence of the switchable ferroelectric polarization. The ability to comprehended and control the sign and strength of DMI by ferroelectric polarization will be a new mechanism to design future nanoscale magnetic devices.

Material and methods

Our first-principles calculations were performed within the framework of Perdew-Burke-Ernzerhof function revised for solids (PBEsol) [52]. The exchange and correlation terms was described by general gradient approximation (GGA) using the Vienna ab initio Simulation Package (VASP) [53]. The core electrons were replaced by the projector augmented wave (PAW) method [54]. The plane-wave kinetic-energy cutoff was 500 eV and the Brillouin zone was sampled on $8 \times 8 \times 8$ and $5 \times 5 \times 1$ Monkhorst–Pack k-points [55] for bulks and HSs, respectively. The criteria of atom force convergence were less than 0.001 eV/Å. The model was described using a periodically repeated in-plane supercells of $\sqrt{2} \times \sqrt{2}$ to explore the magnetic properties and the magnetic exchange coefficient J. A vacuum space of 15 Å along the z direction was adopted to avoid periodic interaction, and it is thick enough to avoid electrostatic interaction (See Supplementary Information). To properly account for the strong Coulomb interaction on the 3d orbitals of Fe ions, the effective onsite Hubbard U correction are set as 5 eV with the Dudarev implementation [56]. Moreover, we consider the spin–orbit coupling during the calculation of the magnetic anisotropy energy (MAE) and DMI. MAE is calculated by the total energy difference between the out-of-plane and the in-plane magnetization system, as shown in the following equation: MAE = E_{001}-E_{100}. Eventually, in order to calculate the DMI, we constructed a $3 \times 2 \times 1$ supercell, and the DMI vector (D) was determined by mapping the total energy of the artificially applied spin configuration on the Hamiltonian [57–59]:

$$H = \sum_{i,j} \boldsymbol{D}_{i,j} \cdot (\boldsymbol{S}_i \times \boldsymbol{S}_j) \tag{1}$$

BFO/BTO HS is composed of tetragonal BTO and tetragonal BFO (both are *P4mm* space group). It has been experimentally evidenced that tetragonal phase can be formed at the HS interface rather than the bulk rhombohedral phase, which has higher ferroelectric polarization [60–62]. Moreover, a stable and robust out-of-plane spontaneous polarization was observed in one-unit-cell-thick BFO films on $SrTiO_3$ substrate [63]. During the simulated epitaxial growth process, the in-plane lattice constant of the BFO/BTO HSs is constrained to the value of the BTO ($a = b = \sqrt{2}a$BTO = 5.65 Å) substrate to simulate epitaxial growth, where BFO ($\sqrt{2}a$BFO = 5.45 Å) contains a 3.5 % tensile strain in the xy-plane. The ionic coordinates are completely relaxed to reach equilibrium. In our calculation, we simulated an idealized abrupt (hard)
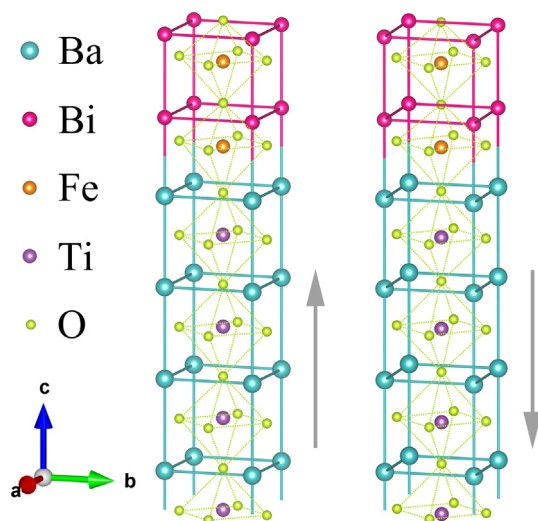
Fig. 1. The schematic crystal structures of the BFO/BTO HSs with different FE polarization direction (gray arrows) of BTO part.

Fig. 2. (a) Total and partial DOS for the bulk BFO. (b) Total and partial DOS for the bulk BTO. The Fermi level is indicated by vertical lines and set to zero.

interface without any defects and atoms diffusion in the HS. Artificial stacking was performed along the (0 0 1) direction for the HSs construction. The BFO/BTO HSs contain 4 monolayers (MLs) of the BTO part, and the bottom two 2 MLs were fixed during the relaxation to simulate a very thick substrate. Note that we would not focus on the properties of these two fixed MLs in the following paper. The FE polarization of the BFO and BTO parts are all assumed to be along the [0 0 1] direction, as shown in Fig. 1. We calculated the interface energy to determine the stability of the HSs, which is defined as the difference between the total energy of HSs ($E_{BTO/BFO}$) and the energy of BTO (E_{BTO}) and BFO (E_{BFO}) part with the same supercell constant, i.e., $E_{ad} = (E_{BTO/BFO} - E_{BTO} - E_{BFO})/A$. Moreover, the area of the interface in the HSs is indicated by $A = 31.92$ Å^2. The aforementioned equation can describe the thermodynamic stability of the interface when the energy released by combining the BTO and BFO parts into a HS. The calculated results show that the E_{ad} values of HSs in $P+$ and $P-$ states are -0.097 eV/Å^2, -0.081 eV/Å^2 respectively, and these negative values indicates that BFO can be epitaxial grown on the BTO substrate stably. It is worth noting that the process of polarization reversal needs to overcome an energy barrier, thus, it will not make the heterostructure spontaneously switch from the one state to the other, even if $P+$ state is more energetically favorable than the other. External electric field as driving force is needed to help the BTO cross the energy barrier, so as to realize the polarization reversal. In addition, the most stable magnetic structure of BFO is determined by collinear magnetic calculation.

Results and discussion

Prior to investigating the controllable magnetic properties by polarization, we first relaxed the bulk structure of BFO and BTO, and calculated the total and the projected density of states (DOS), as shown in Fig. 2. The results show that the bulk BTO is a non-magnetic insulator, as shown in Fig. 2 (b). While for the bulk BFO, the adjacent Fe spins are antiparallel, indicating that the bulk BFO is insulating with G-AFM ordering, as shown in Fig. 2 (a), which are in line with the experiments. In addition, the magnetic moment of Fe ion is 4.15 μB, which is close to the experimental value of 4.34 μB, indicating the rationality of the calculation parameters we used. We then built HS with different polarization states, as shown in Fig. 1. Since we assume that the in-plane lattice parameters of the HSs are the same as those of the BTO substrate,
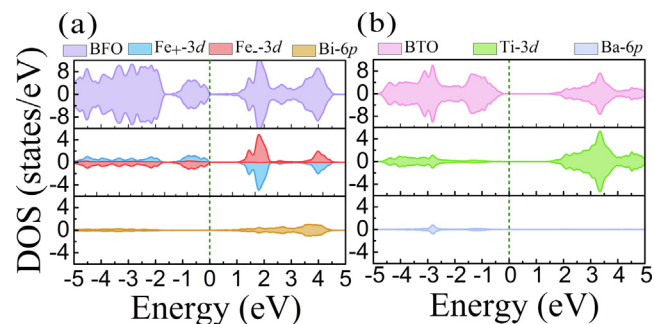
we only analyze the effect of polarization on the lattice parameters of the c direction. We show the change in the lattice parameter of the BFO and BTO part that relative to the bulk in c direction, that is $\Delta C = C_{HS} - C_{bulk}$, as shown in Fig. 4 (b–d). As expected, a comparatively decrease of ΔC occurs on the BFO part rather than the BTO part when they form a HS. Such a reduction can lead to electron reconstruction, then further affecting the properties of BFO part with the presence of substrate polarization.

The calculated various physical properties of the HSs are shown in Table I. It can be clearly seen from the table that the magnetic properties of the BFO can be reversibly switched between AFM and FM ordering with the changing of the BTO two oppositely ferroelectric polarized states. Subsequently, the change between the in-plane and out-of-plane of easy axis occurs simultaneously, indicating that there is a strong and effective ME coupling in the HSs. Experimentally, we can apply an external electric field to drive the polarization reversal, and even if the electric field is removed, the polarization can exist stably. It means that the magnetic properties and the easy magnetization axis can be changed steadily between the two states. Therefore, such a two-dimensional (2D) multiferroic HSs have a promising future as nonvolatile storage material. The way in which materials are electrically write while magnetically read is expected to achieve low power consumption and to greatly improve the storage density of devices. In addition, we compare the anisotropic energy of the HSs with the bulk. Intriguingly, the magnetic anisotropy of the HSs in both polarization states of BTO is greater than the bulk value of BFO, which greatly improves the magnetic stability of the BFO part in the HSs.

In addition, the electrical conductivity of the HS has also changed and a two-dimensional electron gas is formed on the surface of the BFO part. For the perovskite materials, the conductivity and magnetic properties are always coupled together (i.e. coupling between metallicity and FM, insulation and AFM) affected by the indirect exchange between the magnetic atoms. The indirect exchange here refers to the FM double-exchange mediated by itinerant e_g electrons and AFM superexchange mediated by core spins [53]. It is noteworthy that the conductivity always exist in the BFO/BTO HSs in the form of 2D electron gas and do not affected by the appearance of AFM state, which makes the HS a metallic AFM. This provide a greater potential for the application of functional devices based on oxide perovskite materials.

To ensure that the tuning of the properties were not only occurring in the BFO film with specific thickness, we calculated the HSs systems containing different BFO layer thicknesses, and we labeled them as 1n, 2n, 3n, 4n for simplicity according to the number of BFO layers contained in the HSs. The results show that the corresponding properties tuning are all the same as those summarized in Table 1. This indicated that the nonvolatile magnetic control induced by the polarization would not disappear without being affected by the thickness of the BFO layer (for thickness

Table 1
Magnetic properties of the HSs in different polarization states.

	2DMG	magnetic ordering	spin polarizability	MAE (meV)	easy axis
P+	yes	G-AFM	0%	2.74	100
P−	yes	local FM	74%	−2.06	001

Table 2
Magnetic moments (μB) of the Fe atoms and the net magnetization in different numbers of layers for the BTO/BFO HSs. The I-Fe is next to the interface, and the others represents the layers successively away from the interface. Each FeO_2 layer contains two different Fe ions. M indicates the net magnetization contributed from all the ions.

	1n		2n		3n		4n	
+P_{BTO}								
IV-Fe							4.20	−4.20
III-Fe					−4.21	4.21	−4.29	4.29
II-Fe			4.22	−4.22	4.30	−4.30	4.305	−4.305
I-Fe	4.37	−4.37	−4.42	−4.422	−4.43	4.43	−4.426	4.426
M	0		0		0		0	
−P_{BTO}								
IV-Fe							4.02	4.03
III-Fe					4.037	4.023	−4.31	4.25
II-Fe			4.04	4.04	4.25	4.31	4.29	4.30
I-Fe	4.08	4.08	−4.38	−4.32	−4.37	−4.36	−4.36	4.36
M	8.16		8.05		8.01		8.04	

<16.32 Å). Such a result greatly simplify the technological requirements of the HSs fabrication.

The magnetic moments of the HSs with different BFO thicknesses was given in Table 2. The HSs exhibit AFM ordering under the P+ states. While, when it switched to P− states, the local FM ordering appears on the surface of the HSs. This phenomenon applies to all of our BFO/BTO HSs with different BFO thicknesses. Unlike the regular interfacial properties in most other HSs, the change of the magnetic properties in the HSs are directly exposed to the external surface, which makes the device more sensitive to the detection and utilization of magnetism.

The BFO multiferroic material have intrinsic DM interaction (DMI) due to the ferroelectric structure distortion. Such an interaction enables the FM and FE to coupling together, playing a crucial role in determining BFO properties. Therefore, considering the polarization tuning of the magnetism of BFO part, D vector of DMI is an important parameter as well as magnetic exchange J. While J can be determined by mapping the calculated total energies for each magnetic state E_{FM}, E_{AFM1}, E_{AFM2}, E_{AFM3}, as shown in Fig. 4 (a), to the Heisenberg model. (See the Supplementary Information). The exchange coupling constants are then given by the following equation:

$$J_1 = \frac{2E_{AFM1} - E_{AFM2} - E_{FM}}{16S^2} \tag{2}$$

$$J_2 = \frac{2E_{AFM1} - E_{AFM3} - E_{FM}}{16S^2} \tag{3}$$

$$J_3 = \frac{E_{AFM1} - E_{FM}}{4S^2} \tag{4}$$

where J_1 and J_2 is the intralayer nearest neighboring exchange coupling parameter, and J_3 are the interlayer nearest neighboring exchange coupling parameters, S = 5 is the moment. We calculated J and D both for bulk and the HSs, as shown in Table 3. On the one hand, for the interfacial layer of the HSs, we found that the interfacial J value was decreased slightly, while the D vector was greatly enhanced by more than three times compared to the bulk. Especially for the scenarios of P- state, the decrease rate of J value and the increase rate of D vector all are greater than those in the P+ state. This result is expected to provide the D vector a beneficial advantage in the competition with J under polarization tuning, thus possibly inducing the generation of magnetic skyrmion. On the

other hand, for the surficial layer of the HSs, the polarization switching results in the opposite sign of the J value, indicating that there is a magnetic transition between FM and AFM ordering in this layer, which further verifies that the coupling occurs between the polarization and interfacial magnetic ordering. In addition, the change of BTO polarization also led to a 180° switching of the D vector. Therefore, besides the manipulation of magnetic ordering and easy magnetization axis, the polarization can also control the DMI, especially the switching of the D vector at the surface. This greatly enriches the adjustable properties of BTO/BFO HSs with significance for the advancement of the new generation of magnetic device.

To illustrate the underlining physical mechanism of ME coupling, we take 2n HSs as an example to analyze the system in details from an orbital perspective, as shown in Fig. 3. As can be seen intuitively in Fig. 3 (a), 2D electron gas appears on the surface layer of the HSs, which can be interpreted as the FE polarized competition between BFO and BTO part of the HSs. Such a polarization of BFO and BTO part is determined by the displacement between the anions and cations, as shown in Fig. 4. Moreover, this changing regularity of polarization has been confirmed to be applicable to all the HSs with different BFO thickness, as shown in Fig. 4(e–g). The polarization competition shows that, the BFO polarization is always along the −z direction due to the influence of the surface effect. Such a polarization in the −z direction results in the reduction of the electric potential at the surface, which leads to the DOS of the surface layer to pass through the Fermi level, then further facilitating the electrons transfer from the surface to the interior. In addition, the electron transfer is also affected by the polarization of the BTO part. In the P+ state, the polarization direction of the BTO is opposite to that of the BFO part, which weakens the number

Table 3
Density functional theory (DFT) calculation results of the DMI constant (D) and exchange stiffness (J).

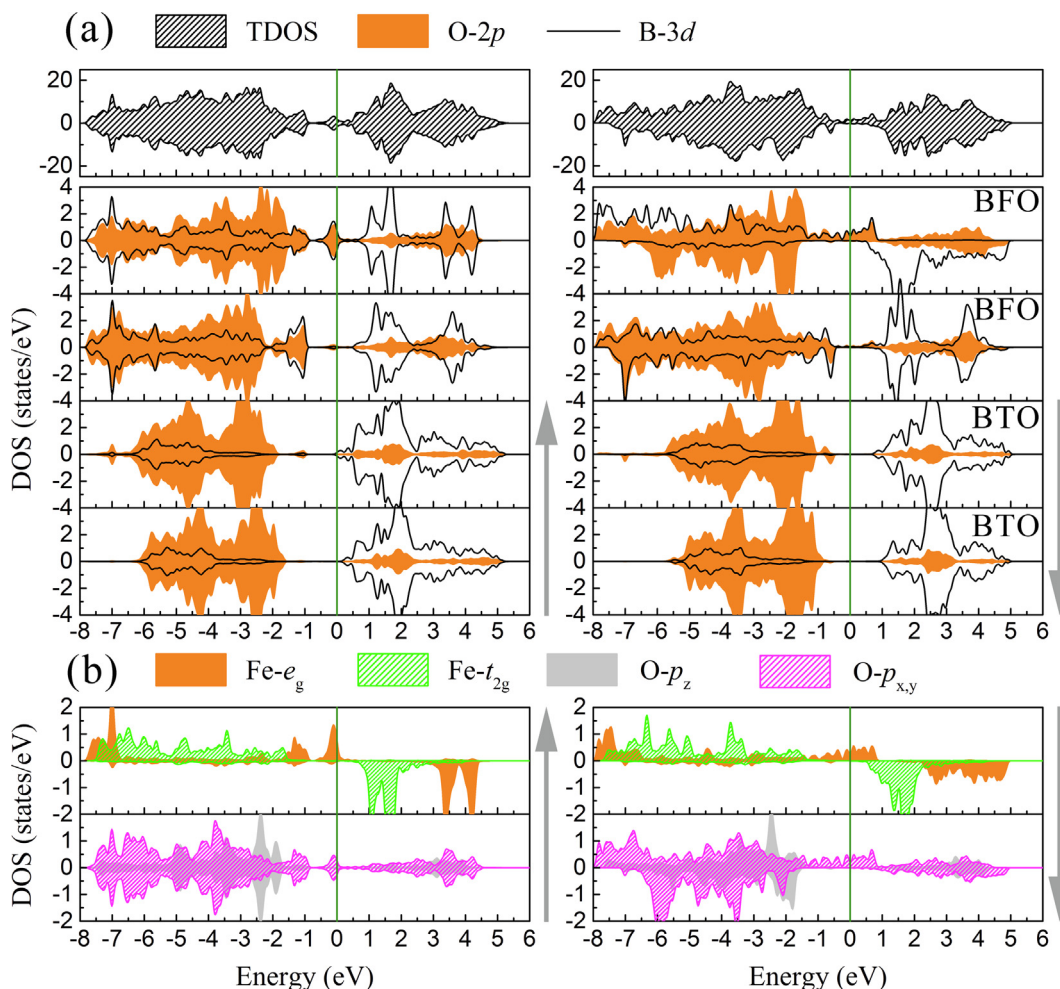|		Interfacial-layer (meV)	Surficial-layer (meV)
J	Bulk	−2.40	−2.40
	P+	−1.56	−0.58
	P−	−1.44	0.87
D	Bulk	−0.24	−0.24
	P+	−0.71	0.15
	P−	−0.82	−0.05

Fig. 3. (a) The total DOS and the layer-resolved partial DOS in different polarization directions for the HSs with 2 BFO MLs. The orange shadowed part represents the O-2p states and the Fe-3d states are represented by black lines. (b) The projected DOS are shown for the surficial FeO$_2$ layer with different FE polarizations direction (gray arrows).

of electron transfer for the BFO part to some extent. While for the *P*- state, the two identical polarization direction greatly enhance the capability of the electron transfer. These results can also be verified by the calculation of the Bader charge.

Different electronic structures at the surface layer affect the magnetic properties of Fe ions under different polarized states. Further analysis were performed on the change of the magnetic ordering from an orbital perspective. As shown intuitively from Fig. 3 (b), the t_{2g} orbitals of the Fe ion are half-filled, while, the spin-down channel of the e_g orbitals are at the unoccupied state. The reversal of the BTO polarization merely affect the e_g electrons of the spin majority states. Such a switch role of polarization leads the e_g spin majority states pass through the Fermi level, resulting in a varying degrees of electron transfer. To quantitatively describe the number of electron transfer, we calculated the electron transfer of Fe-3d orbital in the HSs compared with bulk by integrating the density of states, as shown in Fig. 4 (h). In the *P+* state, only a slight electron transfer occurs in the e_g spin majority states, which makes the Fe-3d orbitals closely remain to being the half-filled high spin d^5 ($t_{2g}^3 \uparrow e_g^2 \uparrow$)state. Therefore, the Fe ions will maintain the superexchange interaction between the Fe^{3+}–O^{2-}–Fe^{3+}, thus, a AFM ordering. For the P- state, the Fe ions maintain a high spin state, but there is a 0.32 electrons transferred emerging in the e_g spin majority states, which results in a mixture state of Fe^{3+} ($t_{2g}^3 \uparrow e_g^2 \uparrow$)and

Fe^{4+} ($t_{2g}^3 \uparrow e_g^1 \uparrow$)in the layer. Additionally, a strong hybridization between the O-$p_{x,y}$ and the Fe-e_g orbitals arises in the, as shown in Fig. 3 (b). This allows the surface to exhibit a local FM ordering through the Fe^{3+}–O^{2-}–Fe^{4+} double exchange effect mediated by the itinerant electron.

Conclusion

In summary, we designed a BFO/BTO HSs to investigate the ME coupling effect using first-principles calculations. We achieved reversible switching of magnetic ordering and easy magnetization axis by switching polarization of BTO. Further analyses reveal that this strong ME coupling is mainly attributed to the different electronic structures caused by the competition between the polarization of BTO and BFO part. In addition, the electron transfer result in the conversion of the surficial exchange interaction from Fe^{3+}–O^{2-}–Fe^{3+} superexchange to Fe^{3+}–O^{2-}–Fe^{4+} double-exchange, then leading a change of the sign for the exchange constant *J*. Remarkably, we found that the magnitude of the DMI in BFO part of the HSs can be increased by three or four times larger than that of the bulk. Furthermore, the nonvolatile control of interfacial DMI vector and the exchange coupling constant are also dominated by the FE polarization. Our work provides a platform for experimental investigating of ME coupling in epitaxial perovskite oxide HSs.
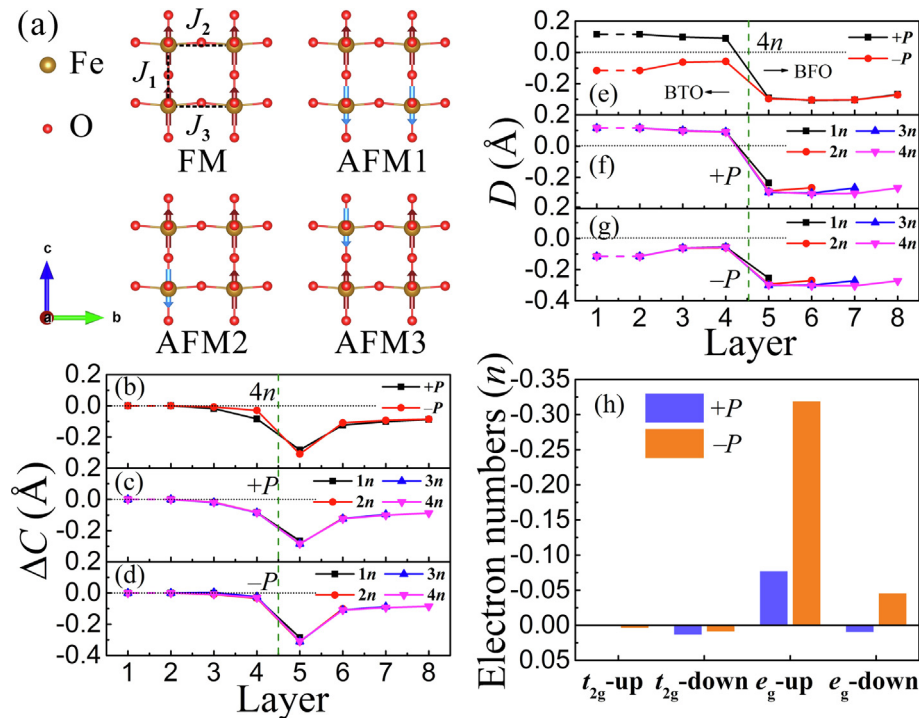
Fig. 4. (a) Four magnetic configurations for the HS with 2 MLs $BiFeO_3$, red and blue arrows are used to distinguish different magnetic directions. The set of J_1, J_2 and J_3 are labeled in the figure. (b–d) The change of the lattice parameter $\Delta C = C_{HS} - C_{bulk}$ that relative to the bulk. The oxygen dimpling away from cations in the z direction for (e) the HSs with 4 BFO MLs, (f) the HSs in the $P+$ states, and (g) P- states with four kinds of BFO MLs. (h) The electron transfer numbers of the Fe-t2g and Fe-eg state at two polarization states.

Declaration of Competing Interest

The authors declare that they have no known competing financial interests or personal relationships that could have appeared to influence the work reported in this paper.

Acknowledgements

Appendix A. Supplementary material

Supplementary data to this article can be found online at https://doi.org/10.1016/j.jare.2020.04.012.

References

[1] Khomskii D. Trend: Classifying multiferroics: Mechanisms and effects. Physics 2009;2:20.
[2] Dong S, Liu J-M, Cheong S-W, Ren Z. Multiferroic materials and magnetoelectric physics: symmetry, entanglement, excitation, and topology. Adv Phys 2015;64(5–6):519–626.
[3] Ramesh R, Spaldin NA. Multiferroics: progress and prospects in thin films. Nat Mater 2007;6(1):21.
[4] Scott J. Data storage: Multiferroic memories. Nat Mater 2007;6(4):256.
[5] Dong S, Xiang H, Dagotto E. Magnetoelectricity in multiferroics: a theoretical perspective. arXiv preprint arXiv:1902.01532; 2019.
[6] Spaldin NA, Fiebig M. The renaissance of magnetoelectric multiferroics. Science 2005;309(5733):391–2.
[7] Eerenstein W, Mathur N, Scott JF. Multiferroic and magnetoelectric materials. Nature 2006;442(7104):759.
[8] Heron J, Bosse J, He Q, Gao Y, Trassin M, Ye L, et al. Deterministic switching of ferromagnetism at room temperature using an electric field. Nature 2014;516 (7531):370.
[9] Hu JM, Chen LQ, Nan CW. Multiferroic heterostructures integrating ferroelectric and magnetic materials. Adv Mater 2016;28(1):15–39.
[10] Wang J, Neaton J, Zheng H, Nagarajan V, Ogale S, Liu B, et al. Epitaxial BiFeO3 multiferroic thin film heterostructures. Science 2003;299(5613): 1719–22.
[11] Cheng ZX. Z Cheng, X Wang, S Dou, H Kimura, K Ozawa, Improved ferroelectric properties in multiferroic BiFeO3 thin films through La and Nb codoping. Phys Rev B 2008;77(9):092101.
[12] Cheng ZX, Wang XL, Du Y, Dou SX. A way to enhance the magnetic moment of multiferroic bismuth ferrite. J Phys D Appl Phys 2010;43(24):242001.
[13] Smolenskii G, Yudin V, Sher E, Stolypin YE. Sov. Phys.-JETP 1963;16:622.
[14] Venevtsev YN, Zhadanov G, Solov'ev S. Sov. Phys.-Crystallogr. 1960;4:538.
[15] Cheng ZX, Li AH, Wang XL, Dou SX, Ozawa K, Kimura H, et al. Structure, ferroelectric properties, and magnetic properties of the La-doped bismuth ferrite. J Appl Phys 2008;103(7):07E507.
[16] Sun W, Wang W, Chen D, Cheng Z, Wang Y. Valence mediated tunable magnetism and electronic properties by ferroelectric polarization switching in 2D FeI 2/In 2 Se 3 van der Waals heterostructures. Nanoscale 2019.
[17] Sun W, Wenxuan W, Chen D, Cheng Z, Jia T, Wang Y. Giant magnetoelectric coupling and two-dimensional electron gas regulated by polarization in BiFeO3/LaFeO3 heterostructures. J Phys Chem C 2019.
[18] Sun W, Wang W, Chen D, Zhang G, Cheng Z, Wang Y. First-principles investigation on tunable electronic properties and magnetism by polarization in PbTiO3/BiFeO3 2D ferroelectric heterostructures. J Mater Chem C 2019;7 (3):463–73.
[19] Cheong S-W, Mostovoy M. Multiferroics: a magnetic twist for ferroelectricity. Nat Mater 2007;6(1):13.
[20] Dong S, Yamauchi K, Yunoki S, Yu R, Liang S, Moreo A, et al. Exchange bias driven by the Dzyaloshinskii-Moriya interaction and ferroelectric polarization at G-type antiferromagnetic perovskite interfaces. Phys Rev Lett 2009;103 (12):127201.
[21] Balk AL, Kim K-W, Pierce DT, Stiles MD, Unguris J, Stavis SM. Simultaneous control of the Dzyaloshinskii-Moriya interaction and magnetic anisotropy in nanomagnetic trilayers. Phys Rev Lett 2017;119(7):077205.
[22] Sergienko IA, Dagotto E. Role of the Dzyaloshinskii-Moriya interaction in multiferroic perovskites. Phys Rev B 2006;73(9):094434.

[23] Soumyanarayanan A, Reyren N, Fert A, Panagopoulos C. Emergent phenomena induced by spin–orbit coupling at surfaces and interfaces. Nature 2016;539 (7630):509.
[24] Meng K-Y, Ahmed AS, Baćani M, Mandru A-O, Zhao X, Bagués NR, et al. Observation of nanoscale skyrmions in SrIrO3/SrRuO3 bilayers. Nano Lett 2019;19(5):3169–75.
[25] Nagaosa N, Tokura Y. Topological properties and dynamics of magnetic skyrmions. Nat Nanotechnol 2013;8(12):899.
[26] Yoshimura Y, Kim K-J, Taniguchi T, Tono T, Ueda K, Hiramatsu R, et al. Soliton-like magnetic domain wall motion induced by the interfacial Dzyaloshinskii-Moriya interaction. Nat Phys 2016;12(2):157.
[27] Heide M, Bihlmayer G, Blügel S. Dzyaloshinskii-Moriya interaction accounting for the orientation of magnetic domains in ultrathin films: Fe/W (110). Phys Rev B 2008;78(14):140403.
[28] Bu K, Kwon H, Kang S, Kim H, Won C. Ordered growth of magnetic helical structure under the Dzyaloshinskii-Moriya interaction. J Magn Magn Mater 2013;343:32–7.
[29] Schmidt L, Hagemeister J, Hsu P-J, Kubetzka A, Von Bergmann K, Wiesendanger R. Symmetry breaking in spin spirals and skyrmions by in-plane and canted magnetic fields. New J Phys 2016;18(7):075007.
[30] Yang H, Boulle O, Cros V, Fert A, Chshiev M. Controlling dzyaloshinskii-moriya interaction via chirality dependent atomic-layer stacking, insulator capping and electric field. Sci Rep 2018:8.
[31] Belabbes A, Bihlmayer G, Bechstedt F, Blügel S, Manchon A. Hund's rule-driven dzyaloshinskii-moriya interaction at 3 d– 5 d interfaces. Phys Rev Lett 2016;117(24):247202.
[32] Srivastava T, Schott M, Juge R, Křižáková V, Belmeguenai M, Roussigné Y, et al. Large-voltage tuning of Dzyaloshinskii-Moriya interactions: A route toward dynamic control of skyrmion chirality. Nano Lett 2018;18(8):4871–7.
[33] Kim N-H, Han D-S, Jung J, Cho J, Kim J-S, Swagten HJ, et al. Improvement of the interfacial Dzyaloshinskii-Moriya interaction by introducing a Ta buffer layer. Appl Phys Lett 2015;107(14):142408.
[34] Fert A, Reyren N, Cros V. Magnetic skyrmions: advances in physics and potential applications. Nat Rev Mater 2017;2(7):17031.
[35] Moon J-H, Seo S-M, Lee K-J, Kim K-W, Ryu J, Lee H-W, et al. Spin-wave propagation in the presence of interfacial Dzyaloshinskii-Moriya interaction. Phys Rev B 2013;88(18):184404.
[36] Yang J-C, Kuo C-Y, Liu H-J, Ding H-C, Duan C-G, Lin H-J, et al. Electrically enhanced magnetization in highly strained BiFeO 3 films. NPG Asia Mater 2016;8(5):e269.
[37] Feng HJ. Electric-field switching magnetization and spin transfer in ultrathin BiFeO3 film. arXiv preprint arXiv:1301.7559; 2013.
[38] Ohuchi Y, Matsuno J, Ogawa N, Kozuka Y, Uchida M, Tokura Y, et al. Electric-field control of anomalous and topological Hall effects in oxide bilayer thin films. Nat Commun 2018;9(1):213.
[39] Yu G, Jenkins A, Ma X, Razavi SA, He C, Yin G, et al. Room-temperature skyrmions in an antiferromagnet-based heterostructure. Nano Lett 2018;18 (2):980–6.
[40] Matsuno J, Ogawa N, Yasuda K, Kagawa F, Koshibae W, Nagaosa N, et al. Interface-driven topological Hall effect in SrRuO3-SrIrO3 bilayer. Sci Adv 2016;2(7):e1600304.
[41] Wang L, Feng Q, Kim Y, Kim R, Lee KH, Pollard SD, et al. Ferroelectrically tunable magnetic skyrmions in ultrathin oxide heterostructures. Nat Mater 2018;17(12):108.
[42] Jochum JK, Lorenz M, Gunnlaugsson HP, Patzig C, Höche T, Grundmann M, et al. Impact of magnetization and hyperfine field distribution on high magnetoelectric coupling strength in BaTiO 3–BiFeO 3 multilayers. Nanoscale 2018;10(12):5574–80.
[43] Gupta R, Chaudhary S, Kotnala R. Interfacial charge induced magnetoelectric coupling at BiFeO3/BaTiO3 bilayer interface. ACS Appl Mater Interfaces 2015;7 (16):8472–9.
[44] Lorenz M, Lazenka V, Schwinkendorf P, Van Bael MJ, Vantomme A, Temst K, et al. Epitaxial coherence at interfaces as origin of high magnetoelectric coupling in multiferroic BaTiO3–BiFeO3 superlattices. Adv Mater Interfaces 2016;3(11):1500822.
[45] Kotnala R, Gupta R, Chaudhary S. Giant magnetoelectric coupling interaction in BaTiO3/BiFeO3/BaTiO3 trilayer multiferroic heterostructures. Appl Phys Lett 2015;107(8):082908.
[46] Lorenz M, Wagner G, Lazenka V, Schwinkendorf P, Bonholzer M, Van Bael M, et al. Correlation of high magnetoelectric coupling with oxygen vacancy superstructure in epitaxial multiferroic BaTiO3-BiFeO3 composite thin films. Materials 2016;9(1):44.
[47] Lorenz M, Hirsch D, Patzig C, Höche T, Hohenberger S, Hochmuth H, et al. Correlation of interface impurities and chemical gradients with high magnetoelectric coupling strength in multiferroic BiFeO3–BaTiO3 superlattices. ACS Appl Mater Interfaces 2017;9(22):18956–65.
[48] Zhang H, Jo W, Wang K, Webber KG. Compositional dependence of dielectric and ferroelectric properties in BiFeO3–BaTiO3 solid solutions. Ceram Int 2014;40(3):4759–65.
[49] Sharma S, Tomar M, Kumar A, Puri NK, Gupta V. Multiferroic BiFeO3/BaTiO3 thin films fabricated by chemical solution deposition technique. MRS Online Proc Library Archive 2015:1805.
[50] Paillard C, Xu B, Dkhil B, Geneste G, Bellaiche L. Photostriction in ferroelectrics from density functional theory. Phys Rev Lett 2016;116(24):247401.
[51] Zhang F, Li M, Zhu Y, Zhao M, Xie S, Wei M, et al. Ferroelectric polarization enhancement of photovoltaic effects in BaTiO3/BiFeO3/TiO2 heterostructure by introducing double-functional layers. J Alloys Compd 2017;695:3178–82.
[52] Perdew JP, Ruzsinszky A, Csonka GI, Vydrov OA, Scuseria GE, Constantin LA, et al. Restoring the density-gradient expansion for exchange in solids and surfaces. Phys Rev Lett 2008;100(13):136406.
[53] Kresse G, Hafner J. Ab initio molecular dynamics for liquid metals. Phys Rev B 1993;47(1):558.
[54] Kresse G, Joubert D. From ultrasoft pseudopotentials to the projector augmented-wave method. Phys Rev B 1999;59(3):1758.
[55] Monkhorst HJ, Pack JD. Special points for Brillouin-zone integrations. Phys Rev B 1976;13(12):5188.
[56] Dudarev S, Botton G, Savrasov S, Humphreys C, Sutton A. Electron-energy-loss spectra and the structural stability of nickel oxide: An LSDA+ U study. Phys Rev B 1998;57(3):1505.
[57] Dzyaloshinsky I. A thermodynamic theory of "weak" ferromagnetism of antiferromagnetics. J Phys Chem Solids 1958;4(4):241–55.
[58] Moriya T. Anisotropic superexchange interaction and weak ferromagnetism. Phys Rev 1960;120(1):91.
[59] Xu C, Xu B, Dupé B, Bellaiche L. Magnetic interactions in BiFeO 3: A first-principles study. Phys Rev B 2019;99(10):104420.
[60] Shao F, Miao J, Wu Y, Xu X, Jiang Y. Multiferroic properties in tetragonal and rhombohedral phase of BiFeO₃/BaTiO₃ heterostructures. INTERMAG 2015. doi: https://doi.org/10.1109/INTMAG.2015.7157316.
[61] Chu YH, Martin LW, Holcomb MB, Ramesh R. Controlling magnetism with multiferroics. Mater Today 2007;10:16–23.
[62] Ederer C, Spaldin NA. Effect of epitaxial strain on the spontaneous polarization of thin film ferroelectrics. Phys Rev Lett 2005;95:257601.
[63] Wang H, Liu ZR, Yoong HY, Paudel TR, Xiao JX, Guo R, et al. Direct observation of room-temperature out-of-plane ferroelectricity and tunneling electroresistance at the two-dimensional limit. Nat Commun 2018;9(1):3319.